Physics – Uspekhi **49** (4) 389 – 399 (2006)

METHODOLOGICAL NOTES PACS numbers: **42.25. – p**, 78.20.Ci, 78.66.Bz

Properties of backward electromagnetic waves and negative reflection in ferrite films

A V Vashkovsky, E H Lock †

DOI: 10.1070/PU2006v049n04ABEH005807

Contents

Abstract. For a backward electromagnetic wave (magnetostatic wave) in a ferrite film, reflection from a perfect mirror formed by the straight edge of the film is investigated experimentally and theoretically. It is found that when the incident wave is collinear (the group velocity vector and the wave vector have opposite directions), negative reflection occurs at any angle of incidence, i.e., the incident and reflected beams are on the same side of the normal to the boundary. It is discovered that a noncollinear backward wave is nonreciprocal in the sense that its energy can be localized both near the surface and in the middle of the film. This property, previously observed only for surface magnetostatic waves, provides both the efficiency of generating and receiving the wave and the possibility of observing the reflected beam. A situation is realized where wave reflection results in two reflected beams. The properties of backward electromagnetic waves propagating in ferrite films are briefly analyzed.

1. Introduction

Recently, extensive research aimed at observing unusual physical effects and phenomena in isotropic media with negative electric permittivity ε and negative magnetic permeability μ has been carried out [1 – 3]. Because natural continuous media with negative ε and μ have not been found, composite materials for observing such effects have been created artificially by alternating layers (or elements) with negative ε and positive μ and layers (elements) with positive ε and negative μ [2]. Until recently, most of the efforts were in fact focused on the study of only one of the unusual physical effects described in Ref. [1], the 'negative refraction,' and its practical applications. At 'negative refraction,' both refracted and incident beams are on the same side of the normal to the boundary, and the applications of this effect include the 'slab superlens,' with its possibility of resolution enhancement, amplification of the so-called 'evanescent' modes, and some others. The analysis of a number of works on this subject can be found in reviews [4, 5]. However, it should be mentioned that although the authors of Refs [2, 3] suggested describing artificial insulators by introducing the effective values of ε and μ, neither ε and μ nor the wavelength inside the composite materials were measured in real experiments, [1] and it was concluded that ε and μ had negative values based on the negative refraction of an electromagnetic wave passing through the composite material. Therefore, the statements that the wavelength of the electromagnetic wave in a composite was much larger than the structure period and that such materials were similar to a continuous medium were only based on theoretical calculations.

At the same time, in some papers [6 – 9], it was suggested that artificial insulators can be described not by introducing the effective electric permittivity and magnetic permeability but by further developing the Brillouin theory [10]. It has been shown that due to the periodicity of such a composite material, if an electromagnetic wave propagating through it has a wavelength comparable with the period of the structure, several refracted waves may appear instead of a single one. Moreover, these refracted waves may propagate on both sides of the normal to the interface between the media [6]. On which side of the normal the refracted wave would then propagate depends on the order of the spatial harmonic and on the ratio between the wavelength and the period of the structure.

Thus, it is evident that the refraction of electromagnetic waves passing through artificial insulators may result in

† The author is also known as E G Lokk. The last name is used in journals adopting the BSI/ANSI transliteration scheme.

A V Vashkovsky, E H Lock Fryazino Branch of the Institute for Radioengineering and Electronics, Russian Academy of Sciences, ul. akad. Vvedenskogo 1, 141190 Fryazino, Moscow region, Russian Federation
Tel. (7-496) 785 56 39 * 13 76. Fax (7-496) 702 95 72
E-mail: edwin@ms.ire.rssi.ru

Received 30 May 2005, revised 5 November 2005
Uspekhi Fizicheskikh Nauk **176** (6) 403 – 414 (2006)
Translated by M V Chekhova; edited by A M Semikhatov

[1] Such measurements were apparently difficult to perform by means of a mobile probe, because the probe could not be translated inside the composite.

several refracted beams, due to the periodicity of the composite material.

However, in order to observe negative refraction and other unusual physical effects, it is not at all necessary to use artificial spatially periodic materials. A number of such effects can be easily observed and studied in continuous anisotropic magnetically ordered media. Due to a large number of different energy interactions existing in these media, such as dipole, exchange, magnetoelastic, and magnetooptic interactions, magnetic crystals and films manifest a variety of unusual physical effects and phenomena, many of which are either impossible in isotropic media (including composite ones) or have principal differences compared with analogous effects in an isotropic medium. For instance, even an ordinary effect such as refraction of electromagnetic waves in an anisotropic medium is substantially different from refraction in isotropic media. Indeed, for the refraction of an electromagnetic wave in a ferrite film, the refractive index is not constant and can take any positive or negative values depending on the angle of incidence [11]. In particular, situations are possible where a wave normally incident on an interface between two media is refracted at a nonzero angle to the normal or a negative refraction occurs with both the incident and the refracted waves being forward waves. [2] Neither of these effects can be observed in isotropic media. As noted in Ref. [11], the reason for negative refraction at the boundary between a vacuum and a medium with negative ε and μ occurs not because ε and μ are negative but because an electromagnetic wave in a medium with negative ε and μ is a backward wave. For a backward wave in an isotropic medium, the momentum direction is opposite to the direction of energy propagation. Therefore, the negative refractive index of a wave propagating through the interface between two media results from the conservation of its tangential momentum component. We note that from the physical standpoint, refraction and reflection of waves in both isotropic and anisotropic media are similar in the sense that the tangent momentum component is conserved. However, the special feature of waves in anisotropic media is that their wavevector **k** and group velocity vector **v** are noncollinear [12]. Because these two vectors correspond to completely different properties, namely, **k** is 'responsible' for the momentum conservation and **v** 'sets' the direction of the beam (energy) propagation, rather unusual cases of refraction and reflection may occur in anisotropic media.

It is known that a ferrite film is one of the few natural media where backward electromagnetic waves can be easily excited and propagate with low losses. However, in contrast to isotropic media, for a backward wave in a ferrite film, the group velocity **v** and the wavevector **k** can be noncollinear. This, in particular, leads to the appearance of backward, or negative, reflection, where both the incident and the reflected beam are on the same side of the normal to the boundary of the medium. This effect cannot be observed in isotropic media. Below, we investigate this effect in detail for backward electromagnetic waves in a ferrite film. In addition, we briefly review the properties of such waves, some of them being described for the first time.

2. Backward electromagnetic waves propagating in ferrite films

We briefly recall what backward electromagnetic waves are and under what conditions they can propagate in a ferrite film.

Let a ferrite film (or slab) of thickness s be magnetized to saturation by a tangent homogeneous magnetic field $\mathbf{H}_0$ (Fig. 1). In both half-spaces outside the film, the magnetic permeability is equal to 1, while the magnetic permeability tensor $\overleftrightarrow{\mu}$ of the film has the form

$$\overleftrightarrow{\mu} = \begin{vmatrix} \mu & \mathrm{i}\nu & 0 \\ -\mathrm{i}\nu & \mu & 0 \\ 0 & 0 & 1 \end{vmatrix}, \tag{1}$$

where

$$\mu = 1 + \frac{\omega_M \omega_H}{\omega_H^2 - \omega^2}\,, \tag{2}$$

$$\nu = \frac{\omega_M \omega}{\omega_H^2 - \omega^2}\,, \tag{3}$$

$\omega_H = \gamma H_0$, $\omega_M = 4\pi\gamma M_0$, $\omega = 2\pi f$, γ is the gyromagnetic constant, $4\pi M_0$ is the saturation magnetization of the ferrite, and f is the electromagnetic oscillation frequency.

Because it is rather difficult to solve the problem of wave propagation in a ferrite film based on the Maxwell equations (in the general case, fourth-order differential equations appear), [3] the dispersion relation for electromagnetic waves is obtained from the Maxwell equations in the magnetostatic approximation:

$$\mathrm{rot}\,\mathbf{h} = 0\,, \tag{4}$$

$$\mathrm{rot}\,\mathbf{b} = 0\,. \tag{5}$$

Equations (4) and (5) can be used for the description of electromagnetic waves because the phase velocity of an electromagnetic wave in a ferrite medium is much less than the speed of light but much larger than the velocity of spin exchange waves. This allows one, on the one hand, to omit the terms $\sim \partial/\partial t$ in the Maxwell equations and, on the other hand, to ignore the terms that take the exchange interaction into account. Because of the use of magnetostatic approximation for their description, electromagnetic waves propagating in ferrites are called magnetostatic waves (MSWs) in the literature [13, 14].

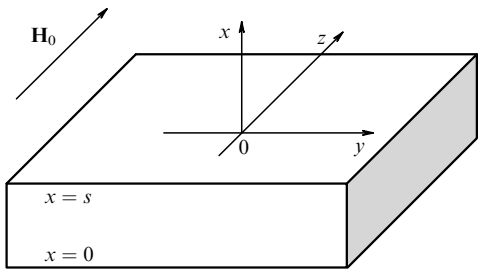

Figure 1. Geometry in which backward electromagnetic waves can be excited in a ferrite film.

[2] The definitions of forward and backward waves for an anisotropic medium are given in Ref. [11].

[3] Analytically, one can only obtain the dispersion relation in the case where the wave propagates along the y axis.

Writing the magnetic induction inside and outside the ferrite slab as $\mathbf{b}_i = \vec{\mu}\,\mathbf{h}_\mathrm{i}$ and $\mathbf{b}_e = \mathbf{h}_\mathrm{e}$, respectively, and introducing the magnetostatic potential Ψ via $\mathbf{h} = \mathrm{grad}\,\Psi$, we can obtain the equations for the potential inside and outside the ferrite plate (Ψ_i and Ψ_e, respectively):

$$\mu\left(\frac{\partial^2\Psi_\mathrm{i}}{\partial x^2}+\frac{\partial^2\Psi_\mathrm{i}}{\partial y^2}\right)+\frac{\partial^2\Psi_\mathrm{i}}{\partial z^2}=0\,, \tag{6}$$

$$\frac{\partial^2\Psi_\mathrm{e}}{\partial x^2}+\frac{\partial^2\Psi_\mathrm{e}}{\partial y^2}+\frac{\partial^2\Psi_\mathrm{e}}{\partial z^2}=0\,. \tag{7}$$

From the continuity conditions for the magnetic induction normal component and the magnetic field tangential components at the interfaces between the ferrite and the two surrounding half-spaces, we obtain the boundary conditions at $x = s$ and $x = 0$:

$$\begin{cases}\mu\,\dfrac{\partial\Psi_\mathrm{i}}{\partial x}+\mathrm{i}\nu\dfrac{\partial\Psi_\mathrm{i}}{\partial y}=\dfrac{\partial\Psi_\mathrm{e}}{\partial x}\,,\\ \Psi_\mathrm{i}=\Psi_\mathrm{e}\,.\end{cases} \tag{8}$$

The solutions for the magnetic potential inside and outside the film (for each half-space) can be written as

$$\begin{cases}\Psi_{1\mathrm{e}} = C\exp(-k_{x\mathrm{e}}x-\mathrm{i}k_y y-\mathrm{i}k_z z)\,,\\ \Psi_\mathrm{i} = \left[A\sin(k_{x\mathrm{i}}x)+B\cos(k_{x\mathrm{i}}x)\right]\exp(-\mathrm{i}k_y y-\mathrm{i}k_z z)\,,\\ \Psi_{2\mathrm{e}} = D\exp(k_{x\mathrm{e}}x-\mathrm{i}k_y y-\mathrm{i}k_z z)\,,\end{cases} \tag{9}$$

where $k_{x\mathrm{e}}$, $k_{x\mathrm{i}}$, k_y, and k_z are the wavevector components along the coordinate axes and A, B, C, and D are arbitrary coefficients. Substituting relations (9) in Eqns (6) and (7), we can express $k_{x\mathrm{e}}$ and $k_{x\mathrm{i}}$ in terms of k_y and k_z:

$$\begin{cases}k_{x\mathrm{i}} = \sqrt{-k_y^2-\dfrac{k_z^2}{\mu}}\,,\\ k_{x\mathrm{e}} = \sqrt{k_y^2+k_z^2}\,.\end{cases} \tag{10}$$

Substituting expressions (9) in boundary conditions (8), we obtain the system of equations

$$\begin{cases}\mu k_{x\mathrm{i}}\left[A\cos(k_{x\mathrm{i}}s)-B\sin(k_{x\mathrm{i}}s)\right]\\ \quad+\nu k_y\left[A\sin(k_{x\mathrm{i}}s)+B\cos(k_{x\mathrm{i}}s)\right] = -k_{x\mathrm{e}}C\exp(k_{x\mathrm{e}}s)\,,\\ \mu k_{x\mathrm{i}}A+\nu k_y B = k_{x\mathrm{e}}D\,,\\ A\sin(k_{x\mathrm{i}}s)+B\cos(k_{x\mathrm{i}}s) = C\exp(k_{x\mathrm{e}}s)\,,\\ B = D\,.\end{cases} \tag{11}$$

Solving system (11), we obtain the following dispersion equation for MSWs propagating in the plane of the film:

$$k_{x\mathrm{e}}^2-\mu^2k_{x\mathrm{i}}^2-\nu^2k_y^2+2\mu k_{x\mathrm{e}}k_{x\mathrm{i}}\cot(k_{x\mathrm{i}}s)=0\,. \tag{12}$$

With the help of relations (10), the components $k_{x\mathrm{e}}$ and $k_{x\mathrm{i}}$ can be eliminated from Eqn (12), which can then be written as

$$(\mu+1)k_z^2+(\mu^2-\nu^2+1)k_y^2 +2\mu\sqrt{\left(-\frac{k_z^2}{\mu}-k_y^2\right)(k_z^2+k_y^2)}\,\cot\left(s\sqrt{-\frac{k_z^2}{\mu}-k_y^2}\right)=0\,. \tag{13}$$

Equation (13) has solutions describing a backward MSW [4] at $k_z \neq 0$ and $\mu < 0$, which is the case within the frequency range $\omega_H < \omega < (\omega_H^2+\omega_H\omega_M)^{1/2}$.

It may seem surprising that although Eqns (12) and (13) have been known for more than forty years, investigations of MSWs were mostly related to the $f(k)$ dependence and the frequency–amplitude characteristic of the transmission coefficient between two transducers in a certain configuration. In this configuration, the two transducers are normal to the magnetic field $\mathbf{H}_0$ and, hence, $k_y = 0$, and the group velocity vector $\mathbf{v}$ is collinear with the wavevector $\mathbf{k}$ (whose absolute value is k_z). [5] Such a configuration was important for creating various filters, delay lines, and other microwave-based devices for analog signal processing. We have reviewed the results of earlier studies with such brevity not to belittle the services of several outstanding researchers but rather to stress that almost no research has been done so far on noncollinear backward waves, which can manifest many unusual physical effects. The only work in this area is Refs [15, 16], where isofrequency (isoenergetic) curves have been calculated. These curves are sections of the dispersion surfaces at $f = \mathrm{const}$ and determine the momentum orientation and the energy propagation direction and, hence, the type of refraction and reflection for a backward wave. At the same time, no attention has been paid in this work to the analysis of refraction or reflection.

3. Characteristics and properties of backward electromagnetic waves propagating in ferrite films

Below, we describe various properties of backward waves and the results of experimental and theoretical studies of reflection in a ferrite yttrium iron garnet (YIG) film on a gadolinium gallium garnet (GGG) substrate. The YIG film was placed in a tangent uniform magnetic field with $\mathbf{H}_0$ 380 Oe and had the magnetization $4\pi M_0 = 1870$ Hz, $2\Delta H = 0.7$ Oe, and thickness $s = 82$ μm. For this thickness, the demagnetizing factor $N \approx 0.007$ must be taken into account; therefore, the value 367 Oe was used for the magnetic field in our calculations. Due to the large s, it was possible to increase the group velocity of volume waves such that a wave could travel a distance of several centimeters without considerable losses. Hence, all phenomena described below could be observed at wave numbers not exceeding $\approx 500\ \mathrm{cm}^{-1}$, which are easily accessible in experiment. In addition, in our earlier work [17], numerical simulations were performed and an agreement was found between the calculated and measured dispersion dependences for the backward and surface MSWs in the same film. These data were used in the present work and provided good agreement between the experimental and theoretical results presented below.

Figure 2 presents isofrequency curves calculated by means of Eqn (13) for a backward electromagnetic wave in the above-described ferrite film. For comparison, the same figure shows orientations of several wave vectors and the

[4] There also exist solutions at imaginary $k_{x\mathrm{i}}$ and $\mu > 0$, which correspond to a forward surface MSW. But this type of MSW is not considered here.
[5] It should be added that other cases have been studied as well, for instance, with a grating of conductive strips placed or grooves etched between the transducers. In addition, the shape of the transducers could be considerably varied.

corresponding group velocity vectors, which are directed normally to the isofrequency curves. Based on the analysis of the isofrequency curves and Eqns (12) and (13), the following properties of backward waves in a ferrite film can be formulated:

Property 1. Backward electromagnetic waves are excited and propagate in ferrite films in the frequency range $f_1 < f < f_2$, where $f_1 = \omega_H/2\pi$ and $f_2 = (\omega_H^2 + \omega_H\omega_M)^{1/2}/2\pi$ are, respectively, the lower and upper frequency limits of the spectrum of backward MSWs.

Property 2. If the wavevector $\mathbf{k}$ of a backward wave is parallel to the magnetic field vector $\mathbf{H}_0$ (to the z axis), then the group velocity vector $\mathbf{v}$ is always directed oppositely to $\mathbf{k}$, and this is the only case where the vectors $\mathbf{k}$ and $\mathbf{v}$ are collinear (as the vectors $\mathbf{k}_1$ and $\mathbf{v}_1$ in Fig. 2, for instance). If the wavevector $\mathbf{k}$ is not parallel to the field $\mathbf{H}_0$ (to the z axis), then the $\mathbf{k}$ and $\mathbf{v}$ vectors of the wave are noncollinear (as the vectors $\mathbf{k_2}$ and $\mathbf{v}_2$, $\mathbf{k}_3$ and $\mathbf{v}_3$, $\mathbf{k}_4$ and $\mathbf{v}_4$ in Fig. 2, for instance). In other words, the wave does not transfer energy along the normal to the phase front in this case. There are no waves for which is normal to the magnetic field vector $\mathbf{H}_0$.

Property 3. Due to the term $\cot(k_{xi}\, s)$ in the dispersion relation, backward waves are multi-mode, i.e., each frequency corresponds to an infinite number of solutions or isofrequency curves.

We note that the multi-mode character of backward waves is considered to be their drawback. It is one of the reasons why there are many fewer works on backward MSWs than on surface MSWs. In this connection, we draw the attention of researchers to the fact that in experiments, it is not difficult to prevent the excitation of higher-order modes by simply choosing the width (or diameter) of the exciting transducer to exceed half the wavelength of the second mode. This method is especially efficient if one works at a fixed frequency or within a relatively narrow frequency range. In what follows, we do not mention the higher-order modes of a backward MSW because they are not excited in the experiments described below. In what follows, the term 'backward MSW' always denotes the first-order mode of a backward MSW.

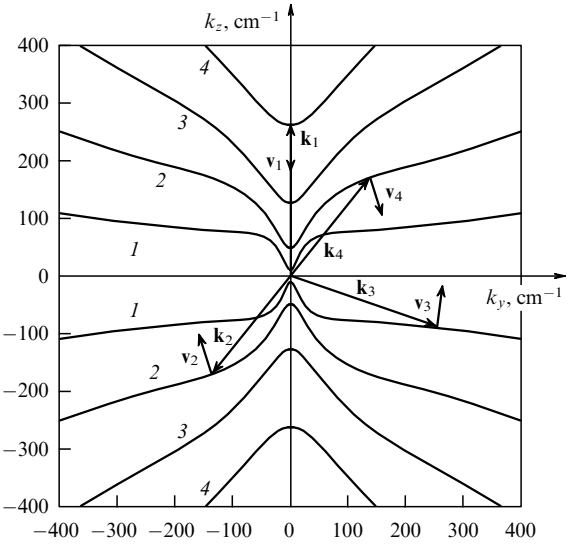

Figure 2. Isofrequency curves of backward electromagnetic waves in a ferrite film for various values of the frequency f: *1* — 2500 MHz, *2* — 2350 MHz, *3* — 2100 MHz, *4* — 1800 MHz. For several arbitrary wavevectors $\mathbf{k}_1$, $\mathbf{k}_2$, $\mathbf{k}_3$, and $\mathbf{k}_4$, orientations of the corresponding group velocity vectors $\mathbf{v}_1$, $\mathbf{v}_2$, $\mathbf{v}_3$, and $\mathbf{v}_4$ are shown.

Above, we have briefly reviewed only those properties of backward waves that had been discovered earlier. However, it turns out that some features of backward MSWs, directly related to reflection and refraction, are so far unknown or have not been considered properly. We therefore consider these features in more detail.

An important characteristic of wave propagation in anisotropic media is the dependence of the group velocity vector $\mathbf{v}$ direction on the wavevector $\mathbf{k}$ direction. Although a general idea of this dependence can be found from the isofrequency curves (Fig. 2), we now show how it can be calculated analytically. The angles ψ and φ giving the orientations of the respective vectors $\mathbf{v}$ and $\mathbf{k}$ are counted from the z axis, which is the symmetry axis for the isofrequency curves of the backward waves. The counterclockwise direction is assumed as the positive direction of the angles. By introducing the relations

$$\begin{cases} k_y = -k\sin\varphi\,, \\ k_z = k\cos\varphi\,, \end{cases} \tag{14}$$

where k is the absolute value of the wave vector in the plane of the film, we can write dispersion relation (13) as

$$\frac{1}{\mu} + \cos^2\varphi + \mu_\perp \sin^2\varphi + 2\alpha\ \cot(\alpha k s) = 0\,. \tag{15}$$

where,

$$\alpha = \sqrt{-\frac{\cos^2\varphi}{\mu} - \sin^2\varphi}\,, \tag{16}$$

$$\mu_\perp = \frac{\mu^2 - \nu^2}{\mu}\,. \tag{17}$$

From (15), we can find the explicit expression for k:

$$k = \Phi(\varphi, f) = \frac{1}{\alpha s}\arctan\left(\frac{-2\alpha}{1/\mu + \cos^2\varphi + \mu_\perp \sin^2\varphi}\right). \tag{18}$$

It is known [16] that the group velocity $\mathbf{v}$ of a wave in an anisotropic medium is defined as the gradient of the frequency in the wavevector space:

$$\mathbf{v} = \mathrm{grad}_k\boldsymbol{\omega} = \frac{\partial\boldsymbol{\omega}}{\partial k_x}\,\mathbf{x}_0 + \frac{\partial\boldsymbol{\omega}}{\partial k_y}\,\mathbf{y}_0 + \frac{\partial\boldsymbol{\omega}}{\partial k_z}\,\mathbf{z}_0\,, \tag{19}$$

where $\mathbf{x}_0$, $\mathbf{y}_0$, and $\mathbf{z}_0$ are unit orthonormalized vectors directed along the corresponding axes. In the case of wave propagation within the yz plane considered here, the angle ψ between $\mathbf{v}$ and $\mathbf{z}_0$ can be easily found from Eqn (19):

$$\psi = \arctan\frac{\partial k_z}{\partial k_y} + n\pi\,. \tag{20}$$

At $n = 0$, the values of ψ correspond to isofrequency curves that are below the k_y axis (for $\pi < \varphi < 2\pi$), and at $n = 1$, to isofrequency curves that are above the k_y axis (for $0 < \varphi < \pi$, see Fig. 2).

Because we are interested in the orientation of $\mathbf{v}$ rather than in its absolute value, we find the partial derivative

$\partial k_z/\partial k_y$ as follows. As can be seen from (18), the dispersion relation for backward waves, $F(k, \varphi, f) = 0$, can be written as

$$F(k, \varphi, f) = k - \Phi(\varphi, f) = 0\,. \tag{21}$$

The derivative $\partial k_z/\partial k_y$ is then given by

$$\frac{\partial k_z}{\partial k_y} = -\frac{\partial F/\partial k_y}{\partial F/\partial k_z} = \left(\frac{\partial F}{\partial \varphi}\,\frac{\partial \varphi}{\partial k_y} + \frac{\partial F}{\partial k}\,\frac{\partial k}{\partial k_y}\right) \times \left(\frac{\partial F}{\partial \varphi}\,\frac{\partial \varphi}{\partial k_z} + \frac{\partial F}{\partial k}\,\frac{\partial k}{\partial k_z}\right)^{-1}. \tag{22}$$

Using expression (21) and the relations $k = (k_y^2 + k_z^2)^{1/2}$ and $\varphi = -\arctan(k_y/k_z)$ obtained from (14), it is easy to find all the derivatives ($\partial F/\partial k = 1$, $\partial F/\partial \varphi = -\partial \Phi/\partial \varphi = -\partial k/\partial \varphi$, $\partial \varphi/\partial k_y = -\cos\varphi/k$, $\partial \varphi/\partial k_z = -\sin\varphi/k$, $\partial k/\partial k_y = -\sin\varphi$, $\partial k/\partial k_z = \cos\varphi$). As a result, Eqn (22) becomes

$$\frac{\partial k_z}{\partial k_y} = \frac{k\,\tan\varphi - \partial k/\partial \varphi}{k + \tan\varphi\,\partial k/\partial \varphi}\,. \tag{23}$$

Calculating the derivative $\partial k/\partial \varphi$ from Eqn (18), we find that

$$\frac{\partial k}{\partial \varphi} = \frac{\sin^2(\alpha k s)\sin(2\varphi)}{2\alpha^2 s}\left[\frac{1}{\alpha}\left(\cot(\alpha k s) - \frac{\alpha k s}{\sin^2(\alpha k s)}\right) \times \left(\frac{1}{\mu} - 1\right) + \mu_\perp - 1\right]. \tag{24}$$

Substituting expression (16) for α in (24) and then (24) in (23) and (23) in (20), we obtain the final relation for the $\psi(\varphi)$ dependence,[6] which gives the orientation of the group velocity vector **v** as a function of the wavevector **k** orientation.

The calculated dependences $\psi(\varphi)$ are presented in Fig. 3. By analyzing Fig. 3, we can formulate another property of backward waves in a ferrite film.

Property 4. For the upper part of the spectrum of backward waves (corresponding to frequencies approximately within the second half of the interval $f_1 < f < f_2$), the dependence $\psi(\varphi)$ is nonmonotonic and has inflections. Therefore, the inverse dependence $\varphi(\psi)$ does not establish a one-to-one correspondence between ψ and φ.

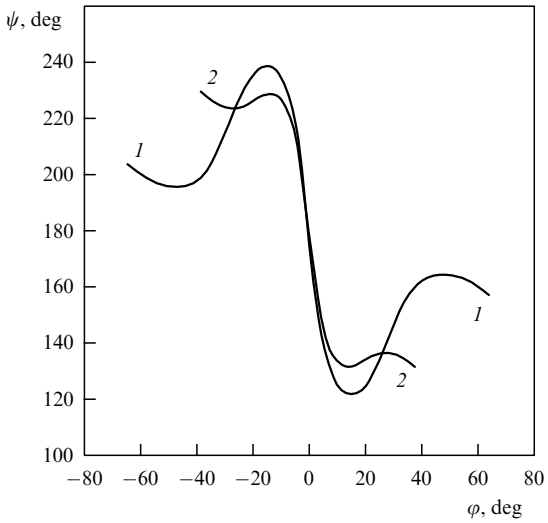

Figure 3. Dependence of the group velocity orientation ψ for the backward wave on its wavevector orientation φ for various values of the frequency f: *1* — 2350 MHz, *2* — 1800 MHz.

[6] The final expression is very bulky and is therefore not presented here.

For instance, the value $\psi = 160°$ is achieved at three values of the angle φ (see Fig. 3, curve *1*): $\varphi_1 = 2°$, $\varphi_2 = 38°$, and $\varphi_3 = 55°$. Therefore, given the beam of a backward wave and, hence, the direction of energy propagation (for instance, $\psi = 160°$), it is not always possible to unambiguously calculate the phase front without knowing where and how the wave was excited. Indeed, the phase front in this case may be oriented at φ_1, φ_2, or φ_3, and it is not clear which of the three directions should be chosen for placing the receiving transducer and detecting the beam. As can be seen from Fig. 2, the isofrequency curve becomes smoother as the frequency decreases, and the dependence $\psi(\varphi)$ becomes monotonic for frequencies $f < 1600$ MHz. We also mote that the angle between the wavevector **k** and the group velocity vector **v** is easily found from Fig. 3 as $\varphi - \psi$.

An important property of backward waves is their nonreciprocality. Researchers who are familiar with the properties of MSWs may argue that backward MSWs do not manifest nonreciprocality and may refer to the works by Damon and Eshbach [13, 14]. In what follows, we show that the nonreciprocality of backward waves occurs as a consequence of the theory [13, 14] but no one has ever paid attention to this fact because, as we have already mentioned, the case of noncollinear backward waves was hardly studied in earlier works.

It follows from the system of equations (11) that the coefficients A, B, C, and D are related as

$$\begin{cases} A = B\,\dfrac{k_{xe} - \nu k_y}{\mu k_{xi}}\,, \\ C = B\left(\dfrac{k_{xe} - \nu k_y}{\mu k_{xi}}\sin(k_{xi}\,s) + \cos(k_{xi}\,s)\right)\exp(k_{xe}\,s)\,, \\ D = B\,. \end{cases} \tag{25}$$

Substituting (25) in (9), we can find the normalized (with respect to B) distribution of the magnetic potential $\Psi(x)$ inside and outside the film. Using Eqns (10) and (14) to eliminate the components k_{xe}, k_{xi}, and k_y from expression (25), we then see that the coefficients A and C depend on the absolute value k of the wavevector, its orientation φ, its frequency, and the parameters of the structure. But it follows from relation (18) that the value φ unambiguously determines the absolute value of k. Therefore, below we analyze the dependences $\Psi(x)$ calculated for various φ values and for the frequency $f = 2350$ MHz (Fig. 4). As can be seen from Fig. 4a, which shows the $\Psi(x)$ dependence for $\varphi = 0$, the magnetic potential distribution is symmetric in this case and the backward wave does not manifest nonreciprocality (a result obtained in Refs [13, 14]). However, at nonzero positive values of φ, the dependence $\Psi(x)$ becomes asymmetric. The second maximum of the potential, which is localized near the $x = 82$ μm surface, gradually decreases and at $\varphi = 21.5°$ becomes only 0.2 times the level of the first maximum, which is localized near the $x = 0$ surface (Fig. 4b, curve *2*). The potential Ψ distribution inside the film bends gradually and eventually looks like a part of the cosine function. For φ larger than 21.5°, the higher maximum of $\Psi(x)$ is localized not near the film surface but inside the film (Fig. 4c, curve *3*). A further increase in φ leads to this higher maximum shifting

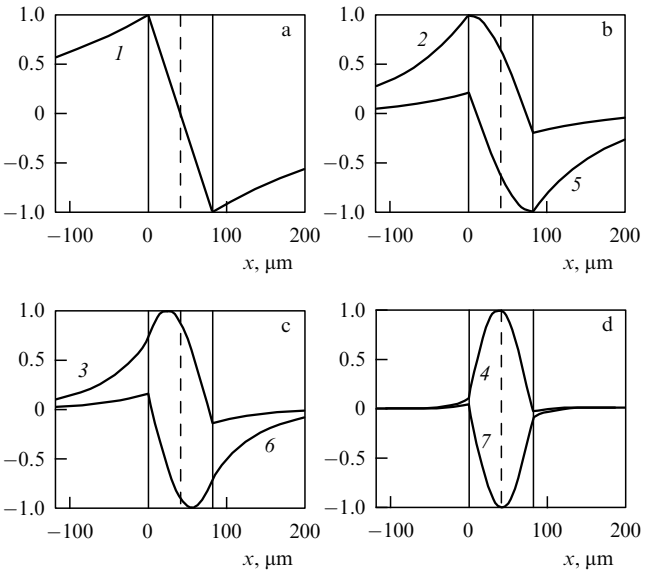

Figure 4. Normalized distribution of the magnetic potential $\Psi(x)$ for various values of the angle φ: *1* — 0°; *2* — −21.5°; *3* — −30°; *4* — −60°; *5* — 21.5°; *6* — 30°, *7* — 60°. Solid vertical lines denote the coordinates of the film surfaces at $x = 0$ and $x = 82$ μm, and the dashed line shows the middle of the film, $x = 41$ μm.

gradually towards the middle of the film (Fig. 4d, curve *4*), and to the further reduction of the lower maximum. At negative values of φ, the dependence $\Psi(x)$ is transformed similarly, with the only (but essential) difference that the higher maximum appears near the $x = 82$ μn surface and the lower one near the $x = 0$ surface (Fig. 4, curves *5*–*7*). This difference in the potential distribution occurs because expressions (25) involve k_y, and changing the sign of this value changes the energy distribution: for $k_y > 0$ ($-180° < \varphi < 0$), the main maximum appears near the upper surface of the film ($x = 82$ μm), and for $k_y < 0$ ($0 < \varphi < 180°$), it appears near its lower surface ($x = 0$).

It is known that an asymmetric potential distribution $\Psi(x)$ leads to the nonreciprocality appearing in the course of wave propagation. We confirmed this fact experimentally by placing two transducers of length 10 mm on the free surface of a film ($x = 82$ μm) such that they excited a backward noncollinear MSW. If the excitation transducer is placed normal to the wavevector $\mathbf{k}_4$ (see Fig. 2), and the receiving transducer, oriented similarly, is moved by a certain distance along the vector $\mathbf{v}_4$ (the line connecting the centers of both transducers must be parallel to $\mathbf{v}_4$), then we can excite and receive a wave beam propagating along $\mathbf{v}_4$. But because the excitation transducer is also normal to the wavevector $\mathbf{k}_2$ (see Fig. 2), another wave beam is excited together with the first one. This second beam travels in the opposite direction, given by the vector $\mathbf{v}_2$. In our experiment, two transducers, with the distance between their centers being 15 mm, excited two wave beams at the frequency $f = 2350$ MHz; for the first beam, the wavevector orientation was $\varphi = -21.5°$, and for the second one, $\varphi = 159.5°$. Because the transducer was placed on the $x = 82$ μm surface, corresponding to the main maximum of the potential $\Psi(x)$ for the first beam (Fig. 4b, curve *5*), the first wave beam was excited efficiently. Indeed, the modulus of the power transmission coefficient was $|K| = -14.2$ dB, the measured damping was $\beta = 0.076$ dB mm^{-1}, and the excitation (and receiving) losses were $\delta = (0.076 \times 15 - 14.2)/2 = -6.53$ dB. The second wave beam was excited inefficiently ($|K| = -40$ dB, $\delta = -19.43$ dB), because the main maximum in the potential $\Psi(x)$ distribution for this beam occurred near the surface $x = 0$ (Fig. 4b, curve *2*), which was at the distance 82 μm from the transducer. We note that for the energy transferred by two beams traveling in opposite directions, the value of $|K|$ at the frequency $f = 2350$ MHz differed by more than 20 dB for orientations of the wavevector within the intervals $-166° < \varphi < -149°$, $-31° < \varphi < -14°$, $14° < \varphi < 31°$, and $149° < \varphi < 166°$.

Thus, based on the calculations and experiments described above, we can formulate other properties of backward waves:

Property 5. The distribution of the magnetic potential $\Psi(x)$ for a backward wave is symmetric when the wavevector $\mathbf{k}$ and the vector $\mathbf{H}_0$ are collinear (at $\varphi = 0$ and $\varphi = 180°$) and asymmetric at other values of φ. For an asymmetric distribution $\Psi(x)$, two cases are possible: a) the main maximum of $\Psi(x)$ is on the surface of the film; b) the main maximum is in the bulk of the film. In both cases, the wave manifests nonreciprocality, in the sense that its excitation and propagation is more efficient in one direction than in the opposite direction. However, one should take into account that when the main maximum is placed close to the middle of the film, the wave is practically impossible to excite in any direction.

Property 6. The study of the magnetic potential distribution $\Psi(x)$ shows that although the z axis, which is parallel to the $\mathbf{H}_0$ vector, is the optic axis, it still has antisymmetric properties, because when each point of the isofrequency curve is reflected with respect to the k_z axis, the $\Psi(x)$ distribution at the symmetric point changes into an antisymmetric distribution (see Fig. 4). The y axis has symmetric properties with respect to the backward wave, because reflection of any point of the isofrequency curve with respect to the k_y axis does not change the potential distribution $\Psi(x)$.

Property 7. The wave beam width d for an electromagnetic wave excited by a transducer of length l is given by

$$d = l\,\frac{|(\mathbf{k}\times\mathbf{v})|}{|\mathbf{k}||\mathbf{v}|} = l\,|\cos(\psi-\varphi)|\,. \tag{26}$$

The values of d are maximal for collinear waves, while for a noncollinear wave, the beam can be rather narrow. For instance, in the experiment described above, the beam width at $\varphi = -21.5°$ was 2.7 times smaller than l. Clearly, formula (26) is valid when the diffraction divergence of the wave beam can be neglected, i.e., in the case where the MSW wavelength λ is small compared to the transducer length l.

4. Reflection of backward electromagnetic waves from the edge of a film

Below, we study the reflection of a backward wave from an perfect mirror, formed in the experiment by a straight polished edge of a ferrite film. A schematic of the experiment in the plane of the ferrite film is shown in Fig. 5, and the parameters of the film are given in Section 3. A surface MSW was excited and detected by mobile antennae whose transducers (*1* and *2* in Fig. 5) were made of gilded tungsten wire of thickness 30 μm and length 10 mm. The transducers were placed on the surface of a YIG film (*3* in Fig. 5), which was

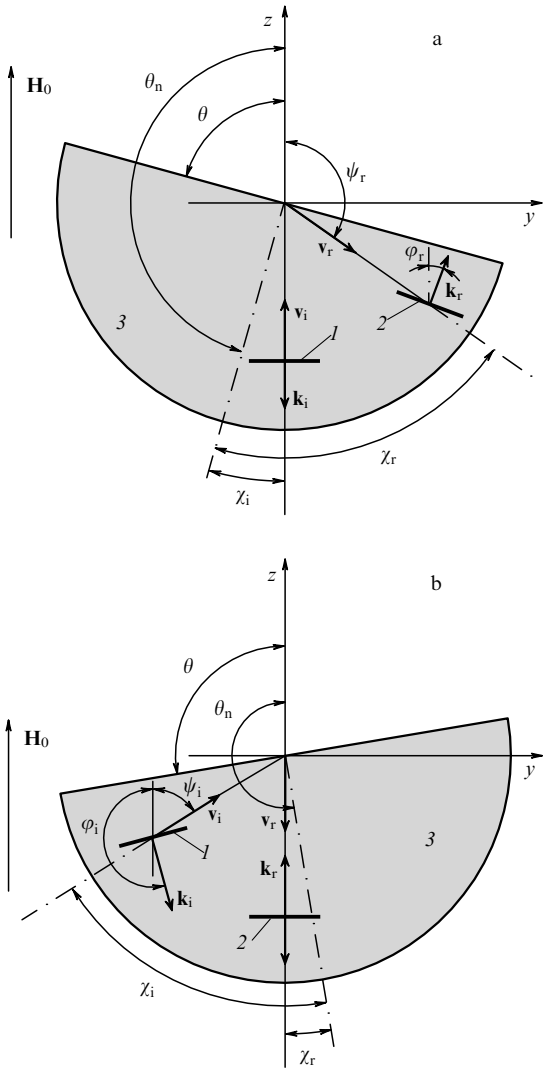

Figure 5. Reflection of a backward wave with the frequency $f = 2350$ MHz (geometry of the experiment in the plane of the film): (a) in the case where the incident wave is collinear and has the parameters $\varphi_i = 180°$, $\psi_i = 0$, $k_i = 47.42$ cm^{-1}, $\lambda_i = 1.325$ mm (reflection is shown for $\theta_n = 165°$, $\theta = 75°$, $\chi_i = 15°$, $\chi_r = -68.5°$, $\varphi_r = -21.5°$, $\psi_r = -126.5°$); (b) in the case where the incident wave is noncollinear and has the parameters $\varphi_i = 195.2°$, $\psi_i = -58.1°$, $k_i = 72.55$ cm^{-1}, $\lambda_i = 0.866$ mm (reflection is shown for $\theta_n = 189.2°$, $\theta = 99.2°$, $\chi_i = -67.3°$, $\chi_r = -9.2°$, $\varphi_r = 0°$, $\psi_r = 180°$).

shaped as a semicircle with the diameter 60 mm. By means of special mechanical apparatuses, both antennae could be moved in the plane of the YIG film and rotated around the axis orthogonal to the film surface. Orientations of the transducers determined the tilt angle of the wavevector $\mathbf{k}$, i.e., provided excitation and detection of waves with a certain vector $\mathbf{k}$. It is convenient to represent the results in a Cartesian frame of reference with the origin (0; 0) coinciding with the center of the YIG film semi-circle, the z axis parallel to the $\mathbf{H}_0$ vector, and the x axis orthogonal to the film surface. The excitation transducer was placed such that the group velocity vector $\mathbf{v}_i$ of the incident wave was directed from the center of the transducer towards the point (0; 0), and the distance between the transducer center and the point (0; 0) was usually within the range 10 – 20 mm (Fig. 5). The position of the excitation transducer was not varied during the measurements, and the incidence angle χ_i was varied by rotating the film around the x axis, which allowed changing the orientation θ of the film boundary. The orientation of the receiving transducer (the angle φ_r) was set, according to calculations, for each new value of χ_i, after which the transducer was moved along the surface of the film to maximize the signal. The direction from the point (0; 0) toward the center of the receiving transducer was assumed to be the measured direction of the group velocity vector for the reflected wave; the angle between this direction and the normal to the film boundary was assumed to be the measured reflection angle χ_r.

We note that in contrast to isotropic media, for which it does not matter whether the dependence $\chi_r(\chi_i)$ is measured by rotating the interface between two media or the excitation antenna, these two ways lead to completely different results for an anisotropic medium. Clearly, the first way, which we actually used, is more convenient, because the parameters of the incident wave (the wavelength λ_i, the vectors $\mathbf{k}_i$, $\mathbf{v}_i$, and the angles φ_i, ψ_i related to them) then remain constant, while for the second way, they depend on the incidence angle (because it determines the orientation of $\mathbf{k}_i$ and $\mathbf{v}_i$ with respect to the vector $\mathbf{H}_0$ of the homogeneous magnetic field).

The angles χ_i, χ_r, and θ were measured by means of a microscope placed above the ferrite film, the origin of the polar frame of reference of the microscope ocular corresponding to the (0; 0) point. The angle χ_i was counted from the normal, [7] and the anticlockwise direction of χ_i was assumed to be positive. The angle χ_r was counted as follows: if the incident and reflected beams were on different sides of the normal, then the sign of χ_r was assumed to be the same as the sign of χ_i; if the incident and reflected beams were on the same side of the normal, the sign of χ_r was assumed to be the opposite of the sign of χ_i. [8] The orientation of the normal, θ_n, and all other angles (orientations of the group velocities and wavevectors for the incident and reflected beams, ψ_i, ψ_r, φ_i, and φ_r) was counted from the z axis, and the anticlockwise direction was assumed to be positive. Clearly, the angles of incidence and reflection of the wave, χ_i and χ_r, and the orientation of the interface between the media, θ, are then related to the angles ψ_i, ψ_r and the orientation of the normal, θ_n, by the simple equations

$$\theta = \theta_n - 90° , \tag{27}$$

$$\chi_i = \psi_i - \theta_n + 180° , \tag{28}$$

$$\chi_r = \psi_r - \theta_n + 360° . \tag{29}$$

As is to become clear from what follows, this definition of the angles is convenient for both describing the reflection and comparing the parameters of the problem in the yz plane and in the wavenumber $k_y k_z$ plane (the isofrequency plane).

In the case where the incident wave vectors $\mathbf{v}_i$ and $\mathbf{k}_i$ are collinear (as in Fig. 5a), characteristics of the reflection are given in Fig. 6, and in the case where the incident wave has noncollinear $\mathbf{v}_i$ and $\mathbf{k}_i$ (as in Fig. 5b), they are given in Fig. 7. Both figures present the experimental and calculated dependences between the reflection and incidence angles, $\chi_r(\chi_i)$, for the frequency $f = 2350$ MHz, and the corresponding depen-

[7] The normal was given by the beam directed normally to the boundary from the (0; 0) point toward the film.

[8] We have to define the reflection angle this way because this definition is commonly used and corresponds to specular reflection, well known for isotropic media, at which the reflection angle is equal to the incidence angle.

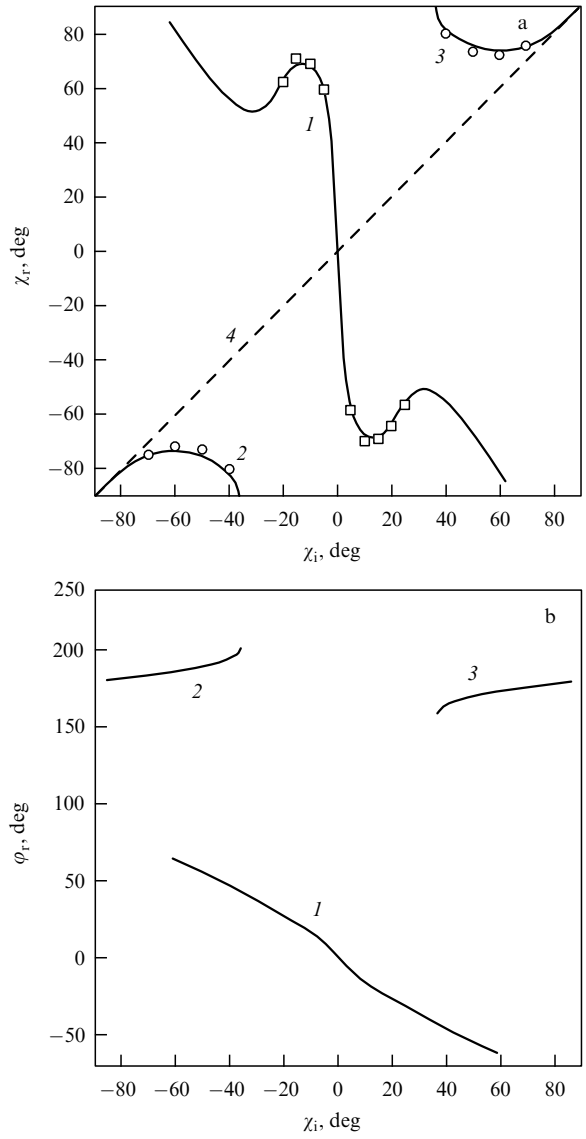

Figure 6. Characteristics of reflection for a backward wave with collinear vectors **k** and **v** and the frequency $f = 2350$ MHz (curves *1–3*); (a) dependence between the reflection angle and the incidence angle, $\chi_r(\chi_i)$ (line *4* corresponds to specular reflection in isotropic media, $\chi_r = \chi_i$); (b) dependence of the orientation of the reflected wave wavevector on the incidence angle, $\varphi_r(\chi_i)$.

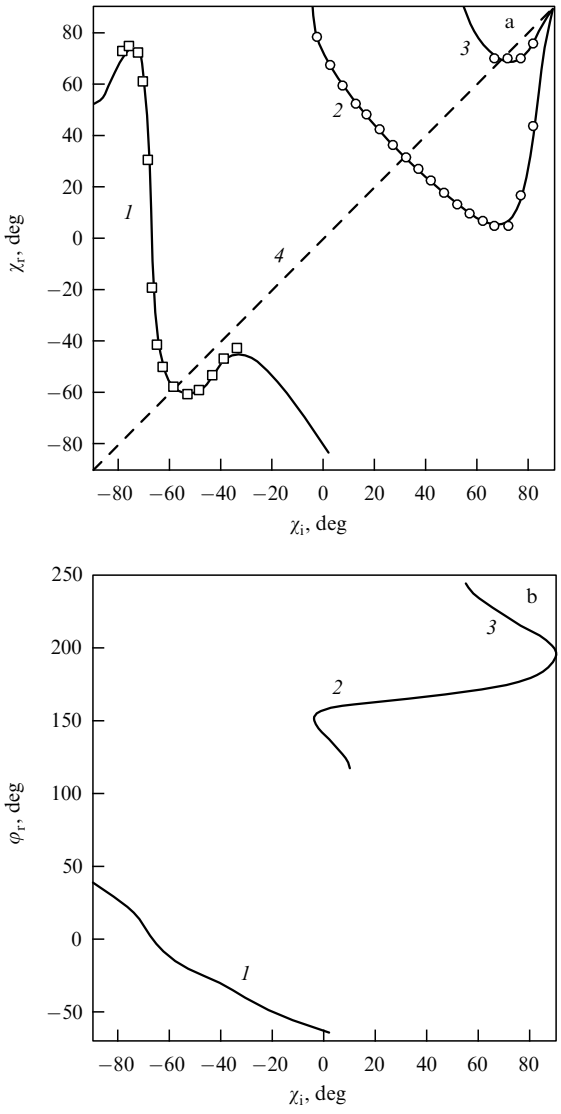

Figure 7. Characteristics of reflection for a backward wave with noncollinear vectors **k** and **v** and the frequency $f = 2350$ MHz (curves *1–3*); (a) dependence between the reflection angle and the incidence angle, $\chi_r(\chi_i)$ (line *4* corresponds to specular reflection in isotropic media, $\chi_r = \chi_i$); (b) dependence of the orientation of the reflected wave wavevector on the incidence angle, $\varphi_r(\chi_i)$.

dences between the orientation of the wavevector **k** of the reflected wave and the incidence angle $\varphi_r(\chi_i)$. As can be seen from Figs 6 and 7, the results obtained demonstrate, on the whole, good agreement between theory and experiment. Because the reflection of waves in anisotropic media essentially differs from the reflection of waves in isotropic media (the $\chi_r(\chi_i)$ dependence for isotropic media is shown in Figs 6 and 7 by dashed line *4*), we comment below on some essential features of the reflection under study.

To make our reasoning more clear, we first consider reflection in the ferrite film by means of geometric constructions in a plane of isofrequency curves (Fig. 8). Because reflection of the waves preserves the momentum (wavevector) component that is tangent to the interface between the media, the wavevector $\mathbf{k}_r$ and the group velocity vector $\mathbf{v}_r$ of the reflected wave can be found as follows. We plot the normal *4* to the interface *3* through the end of the wavevector $\mathbf{k}_i$ of the incident wave, find the point (points) of its intersection with the isofrequency curves, and plot the vectors $\mathbf{k}_r$, $\mathbf{v}_r$ corresponding to this point. In Fig. 8a, where the incident wave is collinear, such constructions are shown in the case where the interface is oriented at $\theta = 75°$. For this value of θ, the normal *4* intersects with only the upper branch *2* of the isofrequency curve. As a result, the incident and reflected beams propagating along the vectors $\mathbf{v}_i$ and $\mathbf{v}_r$ are on the same side of the normal, the reflection angle modulus being larger than the incidence angle modulus, $|\chi_r| > |\chi_i|$. Configuration of the beams in the plane of the film corresponding to Fig. 8a is shown in Fig. 5a. Hereafter, this kind of reflection is called 'negative reflection' for brevity, to be distinguished from 'positive reflection,' where the incident and reflected beams are on different sides of the normal.

Figure 8b, where the incident wave is noncollinear, shows an example of similar constructions in the case where the

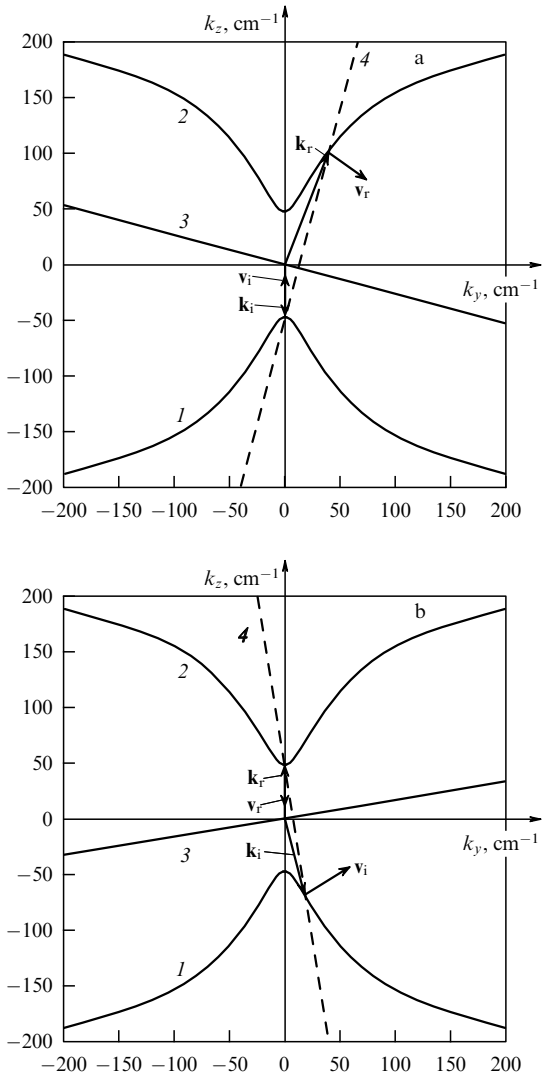

Figure 8. Isofrequency curves of a backward wave with the frequency $f = 2350$ MHz and auxiliary constructions explaining the appearance of negative reflection: (a) the case where the vectors **k** and **v** for the incident wave are collinear (reflection at $\theta = 75°$ is shown); (b) the case where the vectors **k** and **v** for the incident wave are noncollinear (reflection at $\theta = 99.2°$ is shown).

interface is oriented at the angle $\theta = 99.2°$. The beams in the plane of the film are shown in Fig. 5b. In this situation, negative reflection also occurs, the reflected wave being collinear and the modulus of the reflection angle being smaller than that of the incidence angle, $|\chi_r| < |\chi_i|$. Thus, to find the parameters of the reflected wave for every new position of the interface, we must repeat the above-described constructions. (Clearly, it is sufficient to simply rotate the normal around the end of the vector $\mathbf{k}_i$ by a corresponding angle.) It is not difficult to understand that at some orientations of the interface, the normal intersects both the upper (*2*) and lower (*1*) branches of the isofrequency curve in Fig. 8; moreover, two intersections are possible with the latter. This means that, in principle, there may be two or even three reflected beams. However, we must take into account that not every intersection point corresponds to a reflection. Indeed, in real space, in the plane of the film, the vector $\mathbf{v}_r$ must be directed inside the film and not outside it, such that the modulus of the reflection angle, $|\chi_r|$, be less than 90°.

We now return to the discussion of Figs 6 and 7, showing the dependences $\chi_r(\chi_i)$ and $\varphi_r(\chi_i)$. Curves *1* in these figures describe reflection corresponding to the intersection of the normal with the upper branch *2* of the isofrequency curve in Fig. 8 (i.e., with the isofrequency curve that is the opposite of the one describing the incident wave). Curves *2* and *3* in the same figure describe reflections corresponding to the intersection of the normal with the lower branch *1* of the isofrequency curve in Fig. 8 (i.e., with the same isofrequency curve as the one describing the incident wave). Because Figs 6 and 7 provide no information about the angle θ of the interface, we recall that the relation between θ and the incidence angle χ_i can be easily found using formulas (27) and (28). For Fig. 6, where the incident wave is collinear and $\psi_i = 0$, we obtain

$$\theta = 90° - \chi_i\,, \tag{30}$$

and for Fig. 7, where the incident wave is noncollinear and $\psi_i = -58.1°$,

$$\theta = 31.9° - \chi_i\,. \tag{31}$$

Thus, given the values of χ_i, we can find the values of θ. Analyzing Figs 6 and 7, we can formulate another property of backward waves.

Property 8. A collinear backward wave undergoes negative reflection from the interface within the whole range of the angle of incidence χ_i if the incident and reflected waves are described by opposite isofrequency curves. If the incident and reflected waves are described by the same isofrequency curve, positive reflection occurs, which is observed at the incidence angles such that $|\chi_i| > |\chi_{i\,min}|$. Thus, at $|\chi_i| > |\chi_{i\,min}|$, there may appear two reflected beams, with negative and positive χ_r. The value of $\chi_{i\,min}$ depends on the frequency and parameters of the structure (for instance, $\chi_{i\,min} \approx 37°$ in Fig. 6a). A noncollinear wave may undergo negative or positive reflection at the interface, and the type of the reflection strongly depends on the frequency, the parameters of the structure, and the orientation of the wavevector $\mathbf{k}_i$ of the incident wave with respect to the field $\mathbf{H}_0$. In this case, there may also appear two reflected beams.

As can be seen from Fig. 6a, it was not possible to observe both beams in experiments at $|\chi_i| > |\chi_{i\,min}|$. That the reflected beam corresponding to curve *1* in Fig. 6a was not observed at such χ_i can be explained as follows. For $|\chi_i| > |\chi_{i\,min}|$, the wavevector of the reflected wave is at the angle $|\varphi_r| > 40°$ (Fig. 6b, curve *1*) and the distribution of the magnetic potential $\Psi(x)$ for such φ_r has a maximum in the middle of the film. (At the surface, Ψ is very small: see Fig. 4d.) Thus, the sensitivity of our equipment was not sufficient for detecting this reflected beam, localized in the middle of the film, by means of a transducer placed on the surface. This fact, not very optimistic by itself, may be used to derive a more optimistic conclusion:

Property 9. The reflection of a wave from a straight boundary can be used for exciting noncollinear backward waves localized inside the film and collinear waves with symmetric potential distributions (see Figs 4a, d).

Waves that are excited this way and are localized inside the film could be detected by placing another interface on their way, such that reflection would cause a wave with an

asymmetric potential distribution, localized near the external surface (as in Fig. 4b, curve *5*).

As regards collinear waves, their direct excitation by means of a transducer is indeed accompanied by half the power spent on the excitation of a second wave traveling in the opposite direction. This drawback can be eliminated if the waves are excited by means of reflection. We note that it is just because of the excitation of a counter-propagating wave that experimental points with $\chi_i \approx 0$ are absent in Fig. 6a: the weak reflected beam is hard to detect on the background of this wave.

In agreement with the discussion in Section 3 and the reasoning presented above, for a wave to be most efficiently excited in a ferrite film, it should have an asymmetric potential distribution and be localized near the external surface of the film. Characteristics of reflection for such a wave are shown in Fig. 7. Due to a more efficient excitation of the MSW, the amplitude of the reflected wave also increases, which allows the observation of the reflected wave up to the values of $\varphi_r = -40°$ (Figs 7a,b, curve *1*). At the same time, in the case of a collinear MSW, it was possible to detect the reflected wave only up to $\varphi_r = -35°$ (Figs 6a,b, curve *1*). Reflected waves with positive $\varphi_r > 25°$ were not observed (see curves *1* in Figs 6, 7) because the amplitude of the magnetic potential Ψ at the external boundary of the YIG film is very small at such values of φ_r (see Fig. 4b, curve *2*), and the reflected beam is impossible to detect.

For a wave with an asymmetric potential distribution incident at an angle $55° < \chi_i < 90°$ (the orientations of the interface being $-58.1° < \theta < -22.1°$), two reflected beams are observed (Fig. 7, curves *2* and *3*), with all the three waves, the incident and both reflected ones, corresponding to the same isofrequency curve (curve *1* in Fig. 8b).

The dependence $\chi_r(\chi_i)$ in Fig. 7a has three points of specular reflection, corresponding to the points where dashed line *4* intersects curves *1*, *2*, and *3*. Because the reflection angle is equal to the incidence angle for each of these points, the parameters of the reflected wave are completely different in all three cases. These differences are briefly discussed in the property of backward waves formulated below. (Generally speaking, this property is valid for any electromagnetic wave in ferrite films.)

Property 10. In contrast to the case of isotropic media, reflection of waves in ferrite films can manifest three different types of specular reflection. The first type, which corresponds to the intersection between curve *1* and line *4* in Fig. 7a, occurs if the interface is parallel to the y axis ($\theta = 90°$). For this type of reflection, the incident and reflected waves have the same values of wavevectors and group velocities and the same magnetic potential distribution $\Psi(x)$. The second type of specular reflection, which corresponds to the intersection of curve *2* and line *4* in Fig. 7a, occurs when the interface is orthogonal to the optic axis (the z axis), i.e., when $\theta = 0$. For this type of reflection, the incident and reflected waves have the same values of the wavevector and group velocity but different distributions of the magnetic potential $\Psi(x)$. For the incident wave, the main maximum of $\Psi(x)$ is localized near the upper surface of the film, while for the reflected wave, it is close to the lower surface. Thus, both dependences are antisymmetric, as in Fig. 4b, curves *2* and *5*. For the third type of specular reflection, which corresponds to the intersection point of curve *3* and line *4* in Fig. 7a, the incident and reflected waves have completely different values of the wavevector and group velocity and different distributions of the magnetic potential $\Psi(x)$. In this case, there is no direct relation between the orientation θ of the interface and the directions of the symmetry axes; for instance, in Fig. 7a, $\theta = -36°$.

From Fig. 7a, another property of backward waves can be seen.

Property 11. When the beam of a noncollinear wave is normally incident on an interface ($\chi_i = 0$), the reflected beam is not normal to the interface ($\chi_r = 70°$). On the other hand, for a slanting incident beam ($\chi_i = -67°$), the reflected beam may be normal to the interface ($\chi_r = 0$). When the beam of a collinear wave is normally incident on an interface, the reflected beam is also normal to the interface (Fig. 6a).

For a noncollinear incident wave, there may be several ranges of negative reflection. Indeed, in Fig. 7a, these are the intervals $-90° < \chi_i < -67°$ (see curve *1*), $-5° < \chi_i < 0°$ (see curve *2*), and $0° < \chi_i < 5°$ (see curve *1*). With a small variation in the parameters of the wave or the structure, negative reflection can also be observed for $60° < \chi_i < 75°$ (see curve *2*).

We mention several reasons for the observed slight differences between the measured and calculated values of the reflection angles χ_r. First, the value of the homogeneous magnetic field H_0 slightly varied over the ferrite film. As a result, the trajectories of both the incident and reflected beams could be somewhat bent and, hence, errors occurred in the measurement of the incidence and reflection angles. Second, both the incident and the reflected beams had some diffraction divergence. This led to the spreading of both beams and, as a result, to a decrease in the accuracy of tuning to the maximal signal and, hence, in the accuracy of measuring the angles.

Finally, we note that reflection of a backward MSW is essentially influenced by the frequency and the parameters of the film and the incident wave. The effect of all these parameters cannot be considered in the framework of this paper; we therefore tried to describe only the general features of reflection, mainly focusing on the differences between this kind of reflection and the one that occurs in isotropic media.

5. Conclusion

For the reflection of backward electromagnetic waves (magnetostatic waves) from a straight edge of a ferrite film imitating a perfect mirror, characteristic features have been studied experimentally and theoretically. Calculations and measurement results show that in a ferrite film, a situation is possible where both the incident and the reflected beam are on the same side of the normal to the interface, i.e., the reflection is negative, which is impossible in isotropic media. If the wavevector $\mathbf{k}$ and the group velocity vector $\mathbf{v}$ of the incident wave are collinear, negative reflection occurs at any incidence angle; if these vectors are noncollinear, negative reflection can be observed within several intervals of the incidence angle. Within a certain interval of the incidence angle, two reflected waves appeared in experiments. The possibility of observing the reflected beam, as well as the efficiency of exciting and detecting the wave, essentially depended on the distribution of its magnetic potential. In other words, it turned out that a backward wave with noncollinear vectors $\mathbf{k}$ and $\mathbf{v}$ manifests nonreciprocality, which means that the energy of the wave may be localized either near any of the two surfaces or in the middle of the film. A collinear backward wave does not manifest nonreciprocality and has a symmetric (with respect

to the middle of the film) distribution of the magnetic potential. (Historically, this case was the first to be considered, and therefore there was a commonly accepted opinion that backward waves do not manifest nonreciprocality.) In the studies on reflection for backward waves, three various types of specular reflection (when the incidence angle is equal to the reflection angle) can be observed. The first type occurs if the interface is normal to the optic axis, where the incident and reflected waves have the same values of **k** and **v**, and the energies of both waves are localized near the same film surface. The second type occurs if the interface is parallel to the optic axis, then both waves have the same values of **k** and **v**, but the energies of the incident and reflected waves are localized near the opposite surfaces of the film. In the third case, the values of **k** and **v** and the magnetic potential distribution are different for the two waves. In addition, it was discovered that when the beam of a noncollinear wave is normally incident on the interface, the reflected beam is always declined from the normal, while for a slanting incident beam, the reflected beam may be normal to the interface. For a collinear wave, a normally incident beam is always reflected normally to the interface. The properties of backward electromagnetic waves were briefly reviewed, some of them being presented for the first time. It was suggested that waves localized inside the film (whose excitation by means of a transducer is therefore inefficient) be excited using the reflection from the film boundary.

This work was supported in part by the Russian Foundation for Basic Research (grant no. 04-02-16460) and the Program of Basic Research of RAS 'The study of electrophysical phenomena in metamaterials with fluxes of electromagnetic energy.'

References

1. Veselago V G *Usp. Fiz. Nauk* **92** 517 (1967) [*Sov. Phys. Usp.* **10** 509 (1968)]
2. Smith D R et al. *Phys. Rev. Lett.* **84** 4184 (2000)
3. Shelby R A, Smith D R, Schultz S *Science* **292** 77 (2001)
4. Smith D R, Pendry J B, Wiltshire M C K *Science* **305** 788 (2004)
5. Bliokh K Yu, Bliokh Yu P *Usp. Fiz. Nauk* **174** 439 (2004) [*Phys. Usp.* **47** 393 (2004)]
6. Parkhomenko M P, Silin R A, Chepurnykh I P *Radiotekh. Elektron.* **49** 624 (2004) [*J. Commun. Technol. Electron.* **49** 585 (2004)]
7. Silin R A *Voprosy radioelektron. Ser. 1. Elektronika* (4) 3 (1959)
8. Silin R A, Sazonov V P *Zamedlyayushchie Sistemy* (Slowing Structures) (Moscow: Sov. radio, 1966)
9. Silin R A *Periodicheskie Volnovody* (Periodic Waveguides) (Moscow: Fazis, 2002)
10. Brillouin L, Parodi M *Propagation des endes dans les milieux Périodiques* (Paris: Masson, 1956) [Translated into English: *Wave Propagation in Periodic Structures* (New York: Dover Publ., 1953); Translated into Russian (Moscow: IL, 1959)]
11. Vashkovskii A V, Lokk E H *Usp. Fiz. Nauk* **174** 657 (2004) [*Phys. Usp.* **47** 601 (2004)]
12. Born M, Wolf E *Principles of Optics* (Oxford: Pergamon Press, 1964) [Translated into Russian (Moscow: Nauka, 1970)]
13. Damon R W, Eshbach J R *J. Appl. Phys.* **31** S104 (1960)
14. Damon R W, Eshbach J R *J. Phys. Chem. Solids* **19** 308 (1961)
15. Vashkovskii A V et al. *Radiotekh. Elektron.* **32** 2450 (1987)
16. Vashkovskii A V, Stal'makhov V S, Sharaevskii Yu P *Magnitostaticheskie Volny v Elektronike Sverkhvysokikh Chastot* (Magnetostatic Waves in Microwave Electronics) (Saratov: Izd. Saratovskogo Univ., 1993)
17. Lokk E G *Radiotekh. Elektron.* **48** 1484 (2003) [*J. Commun. Technol. Electron.* **48** 1369 (2003)]